Surface structure of domain walls in a ferroelastic system with a domain wall pressure

2002 J. Phys.: Condens. Matter 14 7901

(http://iopscience.iop.org/0953-8984/14/34/308)

INSTITUTE OF PHYSICS PUBLISHING JOURNAL OF PHYSICS: CONDENSED MATTER

J. Phys.: Condens. Matter **14** (2002) 7901–7910 PII: S0953-8984(02)36974-1

Surface structure of domain walls in a ferroelastic system with a domain wall pressure

W T Lee[1,2], E K H Salje[2] and U Bismayer[1]

[1] Mineralogisch-Petrographisches Institut, Universität Hamburg, Grindelallee 48, 20146 Hamburg, Germany
[2] Department of Earth Sciences, University of Cambridge, Downing Street, Cambridge CB2 3EQ, UK

E-mail: wlee@esc.cam.ac.uk

Received 14 May 2002
Published 15 August 2002
Online at stacks.iop.org/JPhysCM/14/7901

Abstract

Previous models of the surface structure of ferroelastic domain walls have neglected one potentially important consideration. This is the effect of a volume strain coupled to the order parameter. Such a coupling affects the structure of the domain wall both in the bulk and at the surface. In the bulk only certain components of the strain tensor can relax in response to the stresses generated within the domain wall by this coupling without disrupting the continuity of the lattice. However, at the surface a more general relaxation is possible. This has an asymmetric effect on the domain wall surface structure, causing it to widen at one surface and narrow at the opposite surface.

1. Introduction

Domain walls occur in many technologically important materials, including ferroelectrics and high temperature superconductors. One important application of domain wall research may be the formation of nanoscopic structures in which dopants are confined to two-dimensional regions by twin walls, as observed experimentally in Na doped WO_3, in which the doping produced two-dimensional superconducting regions inside the domain walls (Aird and Salje 1998, 2000). Obviously the structure of domain walls at the surface will strongly affect the absorption of dopants, so an understanding of the surface structure of domain walls is very important for such applications.

Two previous studies of the surface structure of domain walls have been carried out (Novak and Salje 1998, Conti and Salje 2001). These studies predicted that a domain wall would widen at a surface. However neither study included the effect of couplings between the order parameter (a shear strain) and the dilatational strains. Here we report the results of an investigation into the effect such a coupling has on the surface structure of the domain wall. The results are significantly different from those previously obtained.

Table 1. Interactions in the Novak–Salje model. The first neighbour interaction keeps the values of the a and b lattice parameters close to their bulk values. The second neighbour interaction makes the equilibrium value of the order parameter ε_{12} non-zero and the third neighbour interaction makes sure that the domain walls have finite widths.

		Type of potential
⟨10⟩	First neighbour	Harmonic
⟨11⟩	Second neighbour	Lennard-Jones
⟨20⟩	Third neighbour	Lennard-Jones

The study of Novak and Salje was numerical and consisted of a two-dimensional, square lattice of points which was subjected to potentials causing it to go through a phase transition, the order parameter of which was the shear strain ε_{12}. The functional form of the interaction potentials is given in table 1.

The harmonic potential was chosen to be very strong compared to the Lennard-Jones potential, in order to make the ε_{11} and ε_{22} strains zero. A (01) domain wall was investigated with (10) surfaces, i.e. the domain wall was orthogonal to the surfaces. The observed surface structure of the domain wall was a widening of the domain wall close to both free surfaces. The physical origin of this widening was that the ideal surface value of the strain ε_{12} was different from the ideal bulk value. The relaxation of the surface order parameter profile caused a widening of the domain wall.

Conti and Salje (2001) formulated an analytic analogue of the system studied by Novak and Salje. They linearized the system by performing a Taylor expansion of the free energy about each minimum separately. Their bulk free energy per unit area was

$$F_B = \frac{a}{2}(\varepsilon_{12} \pm \theta)^2 + \frac{b}{2}(\varepsilon_{11}^2 + \varepsilon_{22}^2) + \alpha|\nabla^2 \boldsymbol{u}|^2 \tag{1}$$

with the $\pm$ sign taking opposite values on either side of the domain wall. θ is the bulk value of the shear strain and order parameter in each phase and $\boldsymbol{u}$ is the displacement field.

Their surface free energy per unit length was

$$F_S = \frac{c}{2}(\varepsilon_{12} \pm \phi)^2 \tag{2}$$

where ϕ is the value of the surface order parameter far from the wall.

The minimization of the above free energy with the boundary condition $\varepsilon_{12} = 0$ at the centre of the domain wall gives results similar to those obtained by the numerical simulation of Novak and Salje but allowed for a wider exploration of parameter space.

The two models described above neglect an important consideration in determining the bulk and surface structure of domain walls. This is the possibility of coupling terms in the free energy between the dilatational strains ε_{11} and ε_{22}, and the order parameter ε_{12}. From the symmetry of the high temperature phase the lowest order coupling term must be quadratic in the order parameter and linear in the dilatational strains. The effects of this coupling are excluded from both the model of Novak and Salje, and the model of Conti and Salje. In the Novak–Salje model the coupling does exist, but the harmonic interactions are so strong that this coupling term has no measurable effects. In the Conti–Salje model the expansion of the free energy in terms of the strains is only taken to second order, thus the coupling term, which is third order, is excluded.

The aim of this study is to investigate the effect of this coupling term on the surface structure of the domain wall. Therefore we consider a numerical model similar to the Novak–Salje model but with the nearest neighbour interaction strength reduced to a physically reasonable value. The parameters of the system are adjusted so that the ideal bulk and surface values of the order parameter are as close to each other as possible, so that the mechanism of domain wall

widening seen in the two models discussed above will not operate and only the effect of the coupling will be observed. In general, of course, both mechanisms will operate together.

The results of the numerical simulations are different from those observed in the Novak–Salje and the Conti–Salje models. In this case the three components of the two-dimensional strain tensor take non-zero values. The domain wall widens at one surface and narrows at the other surface. This is different from the results of the previous two studies where the strain profile of the domain wall is symmetrical at the two surfaces.

The physical origin of the surface relaxation of the domain wall is as follows. The coupling between the dilatational strains and the order parameter can be considered as a domain wall pressure; i.e. when the value of the order parameter deviates from its ideal bulk value there is a resulting internal pressure (the pressure can be positive or negative, depending on the sign of the coupling). Far from a free surface only the component of the strain perpendicular to the surface can relax: if the dilatational strain parallel to the domain wall deviates from its bulk value the continuity of the crystal structure will be disrupted. So in the bulk of the crystal the order parameter ε_{12} takes the hyperbolic tangent form for an order parameter across a domain wall. Inside the domain wall the strain ε_{11} takes a non-zero value, but the strain ε_{22} remains zero, despite the fact that the domain wall pressure is isotropic.

What happens at the surface may be considered in perturbation theory, where the small parameter is the coupling coefficient. To first order the domain wall pressure causes displacements of the atoms perpendicular to the surface. This makes the surface value of ε_{22} non-zero, but symmetrical with respect to the two surfaces. However, because the magnitude of the displacement perpendicular to the surface depends on the coordinate parallel to the surface, the displacement perpendicular to the surface also affects ε_{12}. In fact the effect is to make ε_{12} asymmetrical at the two opposite surfaces.

In second order perturbation theory, because ε_{12} has been changed, the domain wall pressure is also changed. The resulting domain wall pressure is asymmetrical and thus ε_{11} and ε_{22} become asymmetrical as well as ε_{12}. Therefore the effect of a coupling between the order parameter and the dilatational strain is to produce an asymmetric domain wall profile, with all the components of the strain tensor showing different behaviours at opposite free surfaces.

The rest of the paper is divided into three sections. In the first of these sections we describe a numerical investigation into the surface structure of domain walls with coupling between the dilatational strain and the shear strain. The model used is similar to the Novak–Salje model but with different interactions. In the next section we describe an analytic investigation of the simplest possible free energy functional which describes the system. The first order form of the surface profile can be calculated from such a free energy, but the second order correction is too complicated. Instead we approximated the system by an isotropic elastic medium with surface forces acting upon it. This model qualitatively reproduces the domain wall profile given by the numerical calculations.

2. Numerical studies of the surface structure of the domain wall

In this section we describe our numerical investigation of a system with coupling between the order parameter and dilatational strains. An investigation of such a system with no free surfaces has been carried out by Lee *et al* (2001) with the aim of determining the effect of the domain wall structure on the transport properties. The model consists, in its high temperature form, of a tetragonal lattice with the a and c lattice parameters set equal. The forms of the interaction parameters are as given in table 2.

Only one of the interactions is anharmonic: the minimum necessary for a phase transition to occur. The coupling of the strains ε_{12} and ε_{11} and ε_{22} is proportional to q_3. At the surface

Table 2. Interactions used in the numerical model. As can be seen nearly all the interactions used are harmonic. Only the second neighbour interaction is anharmonic: at least one interaction must be anharmonic or the system will not have a phase transition.

	In plane interactions	
⟨100⟩	Harmonic	$f_{100} = \frac{k_1}{2}(r - a_1)^2$
⟨110⟩	Anharmonic	$f_{110} = -\frac{q_2}{2}(r - \sqrt{2})^2 + \frac{q_3}{3}(r - \sqrt{2})^3 + \frac{q_4}{4}(r - \sqrt{2})^4$
⟨200⟩	Harmonic	$f_{200} = \frac{k_3}{2}(r - a_3)^2$
	Out of plane interactions	
⟨001⟩	Harmonic	$f_{001} = \frac{k_1}{2}(r - 1)^2$
⟨101⟩	Harmonic	$f_{101} = \frac{k_1}{2}(r - \sqrt{2})^2$

Table 3. Values of the parameters of the interaction functions used in the numerical study.

Coefficient	Value
k_1	50.0
k_3	−0.665
q_2	2.500
q_3	−200.0
q_4	1.82×10^3
a_1 (bulk)	0.830
a_1 (surface)	0.912
a_3	−4.920

a different value of a_1 is used for the [010] interaction so that the ideal surface value of ε_{12} is the same as the ideal bulk value. The numerical values of the coefficients used are given in table 3.

The system size was 20 by 40 by 5 atoms. Periodic boundary conditions were employed except at the free surfaces. The relaxed configuration of half the system is shown in figure 1. A schematic diagram of the system is shown in figure 2, indicating the part of the system used to generate plots. Plots of the components of the strain tensor are shown in figure 3. Instead of showing two ends of a domain wall these plots show two adjacent domain walls intersecting the same surface. These show clearly that the strain profiles of the two domain walls are quite different.

Figure 4 shows graphs of ε_{11}, ε_{22} and ε_{12} at the surfaces and in the centre of the system. These clearly show the asymmetrical change in shape of the domain wall at each surface: one domain wall widens close to the surface and the other narrows.

3. Analytical investigation of the surface structure of the domain wall

To check our understanding of the mechanism of asymmetric domain wall formation we investigated the simplest possible free energy per unit length that reproduced the numerical results. This was

$$F = \int \left[-\frac{A}{2}\varepsilon_{12}^2 + \frac{1}{4}\varepsilon_{12}^4 + \frac{B}{2}(\varepsilon_{11}^2 + \varepsilon_{22}^2) + \lambda\varepsilon_{12}^2(\varepsilon_{11} + \varepsilon_{22}) + \frac{1}{2}\left(\frac{\partial\varepsilon_{12}}{\partial x}\right)^2 \right] \mathrm{d}^2 r. \tag{3}$$

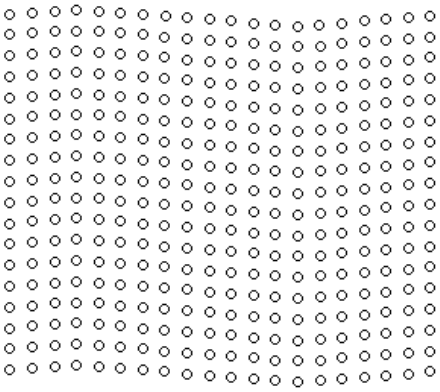

Figure 1. This shows the configuration of half the system. The upper edge is a free surface but the lower edge lies within the bulk. The system has two vertical domain walls. The x-axis is horizontal; the y-axis is vertical.

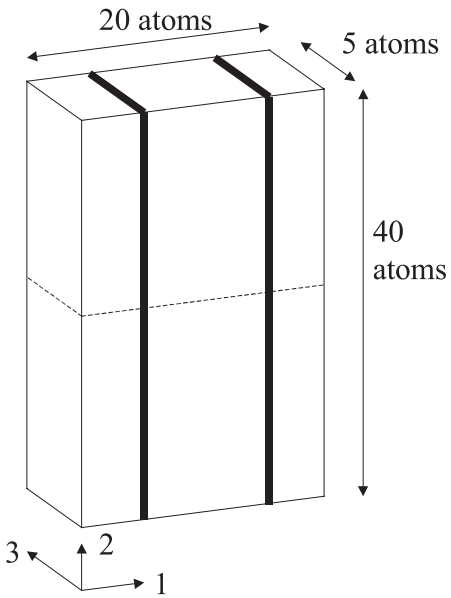

Figure 2. The system we investigated consisted of a ferroelastic lattice with two domain walls (bold lines). Only the half of the system above the dotted line is shown in the figures.

There are many terms which are required by symmetry in equation (1) which have been omitted for simplicity. Even so we were only able to calculate the domain wall profile from it to first order in perturbation theory. Since the second order term was necessary to obtain results qualitatively similar to those seen in the numerical simulations a different method had to be adopted to calculate these.

The elements of the stress tensor can be calculated from this free energy by $\sigma_{ij} = \delta F/\delta\varepsilon_{ij}$. The equations describing the equilibrium of the bulk in the absence of body forces are $0 = \partial\sigma_{ij}/\partial r_j$ (Landau and Lifshitz 1986). If there is a free surface, with unit normal $\boldsymbol{n}$, the boundary conditions are $0 = n_j\sigma_{ij}$.

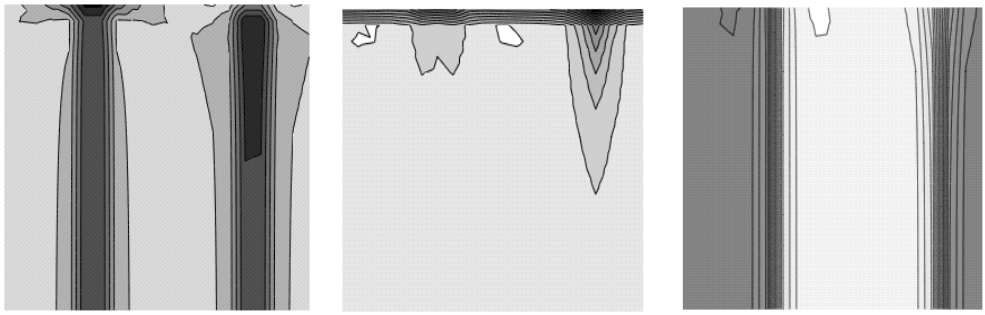

(a) ε_{11} (b) ε_{22} (c) ε_{12}

Figure 3. Strains in the configuration shown in figure 1. These clearly show that the two surface structures of the domain wall are not equivalent.

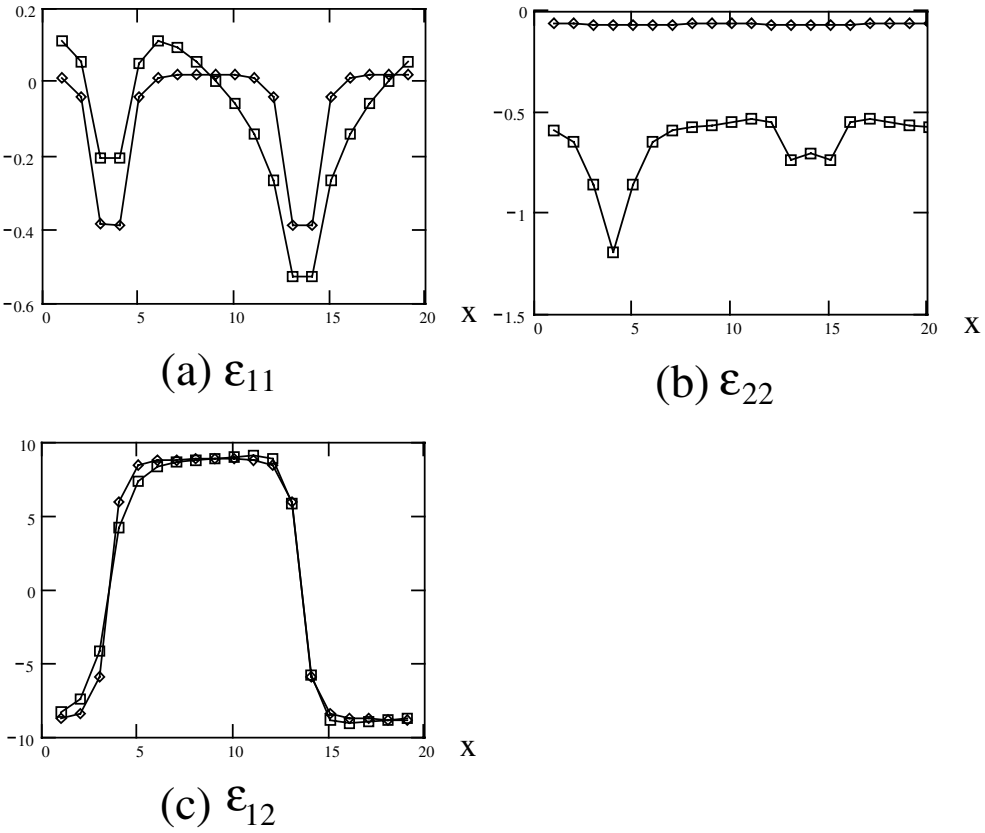

Figure 4. Strains at the surface and in the domain wall. Boxes correspond to the surface and diamonds to the bulk. These plots show that the domain wall widens at one surface and narrows at the other.

Firstly we consider the case of a domain wall parallel to the y-axis, with no free surfaces. In this case the solutions to the bulk equilibrium equations are, to lowest order in the coupling constant λ,

$$\begin{aligned}\varepsilon^b_{11} &= -\frac{\lambda A}{b}\tanh^2\left(\frac{x}{w}\right)\\ \varepsilon^b_{22} &= -\frac{\lambda A}{B}\\ \varepsilon^b_{12} &= \sqrt{A}\tanh\left(\frac{x}{w}\right)\end{aligned} \tag{4}$$

where $w = \sqrt{2/A}$. The only element of the stress tensor that is non-zero in this case is σ_{22} which is

$$\sigma_{22} = A\lambda\tanh^2\left(\frac{x}{w}\right). \tag{5}$$

This stress does not cause any displacements at the bulk but at the surface it will cause displacements. To determine these we solve the equilibrium equations to first order in lambda with one free surface. We assume that the solution is separable, and solve the resulting equations in the region close to the domain wall. That is, we write for the additional displacement due to the presence of the surface $u_x(x, y) = u^x_x(x)u^y_x(y)$ and $u_y(x, y) = u^x_y(x)u^y_y(y)$. Then the components of the strain tensor become

$$\begin{aligned}\varepsilon_{11} &= \varepsilon^b_{11} + \frac{\partial u^x_x(x)}{\partial x}u^y_x(y)\\ \varepsilon_{22} &= \varepsilon^b_{22} + u^x_y(x)\frac{\partial u^y_y(y)}{\partial y}\\ \varepsilon_{12} &= \varepsilon^b_{12} + \left(u^x_x(x)\frac{\partial u^y_x(y)}{\partial y} + \frac{\partial u^x_y(x)}{\partial x}u^y_y(y)\right).\end{aligned} \tag{6}$$

The surface equations can be solved to give $u^x_x(x)$ and $u^x_y(x)$. To obtain $u^y_x(y)$ and $u^y_y(y)$ and make the separable solution valid we solve the bulk equations in the limit of small x. Therefore the solutions obtained in this way are valid close to the surface and close to the domain wall. We also made use of the fact that for a system which undergoes a shearing ferroelastic transition $a \ll b$.

The resulting values of the elements of the strain tensor are

$$\begin{aligned}\varepsilon_{11} = \varepsilon^b_{11} &- \frac{A}{2B(3A+4B)}\left[4B\exp\left(-2y\sqrt{\frac{2B}{3}}\right) + 3A\exp\left(-Ay\sqrt{\frac{3}{2}}\right)\right]\\ &\times\left[3\tanh^2\left(\frac{x}{w}\right) - 1\right]\left[\tanh^2\left(\frac{x}{w}\right) - 1\right]\\ \varepsilon_{22} = \varepsilon^b_{22} &- \frac{A}{2B(3A+4B)}\left[3A\exp\left(-2y\sqrt{\frac{2B}{3}}\right) + 4B\exp\left(-Ay\sqrt{\frac{3}{2}}\right)\right]\\ &\times\left[\tanh^2\left(\frac{x}{w}\right) - 1\right]\\ \varepsilon_{12} = \varepsilon^b_{12} &- \frac{\sqrt{A}(16B^2+9a^2)}{2\sqrt{3B^3}(3A+4B)}\left[\exp\left(-2y\sqrt{\frac{2B}{3}}\right) + \exp\left(-Ay\sqrt{\frac{3}{2}}\right)\right]\\ &\times\left[\tanh^2\left(\frac{x}{w}\right) - 1\right]\tanh\left(\frac{x}{w}\right).\end{aligned} \tag{7}$$

These results are not qualitatively similar to the numerical results. The strains ε_{11} and ε_{22} remain symmetrical and only the shear strain ε_{12} becomes asymmetric. The resulting strains at the surface are shown in figure 5. The values of the parameters used are $A = 1$, $B = 10$ and $\lambda = -1.5$.

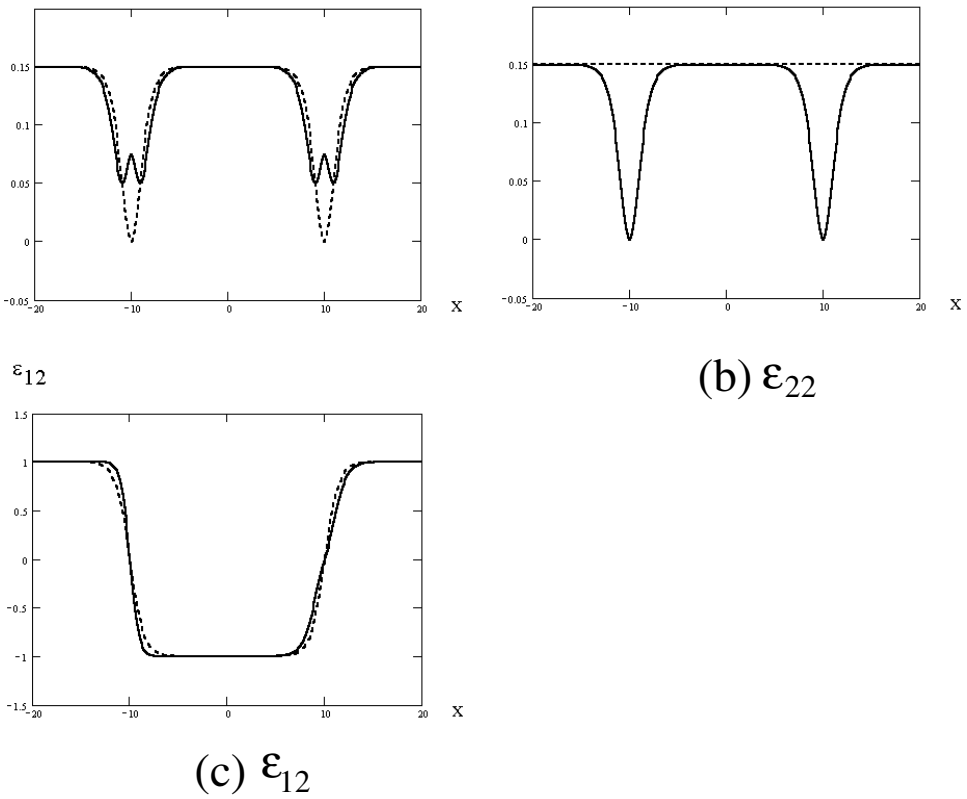

Figure 5. Strains at the surface and in the bulk calculated from equation (7). Dotted curves give the bulk values and the solid curve gives the surface value. Only the asymmetry in ε_{12} is reproduced. The asymmetry in ε_{11} and ε_{22} must be given by higher order perturbation theory.

Table 4. Forces, and points of action of the forces, shown in figure 6. x is the horizontal coordinate of the point of action of the force, relative to the centre of the domain wall. F/E is the magnitude of the force divided by the Young's modulus of the material. $f_{1–4}$ are vertical and have the same sign in each domain wall. f_5 is horizontal and has opposite signs in the two domain walls.

	x	F/E
f_1	0	0.50
f_2	0.5	0.25
f_3	1.0	0.07
f_4	1.5	0.03
f_5	0.5	1.0

Now that the strain ε_{12} is asymmetric it is clear that at the next order of perturbation theory the coupling between ε_{12} and ε_{11} and ε_{22} will ensure that ε_{11} and ε_{22} are asymmetrical. Unfortunately calculating the second order of perturbation theory proved too complicated so we resorted to an alternative means of calculating the surface strains.

We replaced the system by an isotropic elastic medium, and replaced the effects of the internal stresses by forces acting on the surface. How this is done is shown in figure 6. The

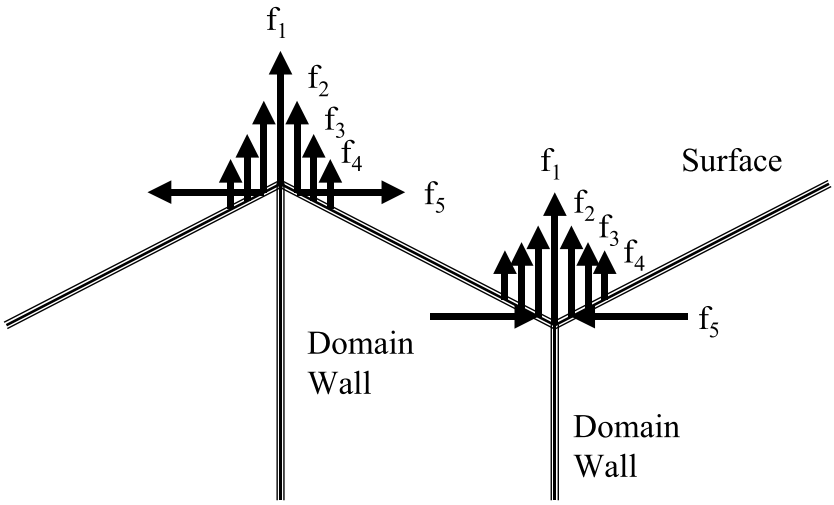

Figure 6. Diagram showing the forces and their points of application used in calculating the second order strains.

system with the bulk strains from equation (4) embedded in it is treated as an elastic medium. The effects of the internal stresses are taken into account by replacing them by surface forces as shown in figure 6. The magnitudes and points of action of the forces are given in table 4. The displacements caused by a surface force are given by (Landau and Lifshitz 1986)

$$\begin{aligned}
u_x &= \frac{1+\sigma}{2\pi E}\left\{\left[\frac{xz}{r^3}-\frac{(1-2\sigma)x}{r(r+z)}\right]F_z+\frac{2(1-\sigma)r+z}{r(r+z)}F_x+\frac{[2r(\sigma r+z)+z^2]x}{r^3(r+z)^2}(xF_x+yF_y)\right\}\\
u_y &= \frac{1+\sigma}{2\pi E}\left\{\left[\frac{yz}{r^3}-\frac{(1-2\sigma)y}{r(r+z)}\right]F_z+\frac{2(1-\sigma)r+z}{r(r+z)}F_x\right.\\
&\qquad\left.+\frac{[2r(\sigma r+z)+z^2]y}{r^3(r+z)^2}(xF_x+yF_y)\right\}\\
u_z &= \frac{1+\sigma}{2\pi E}\left\{\left[\frac{z^2}{r^3}-\frac{2(1-\sigma)}{r}\right]F_z+\left[\frac{1-2\sigma}{r(r+z)}+\frac{z}{r^3}\right](xF_x+yF_y)\right\}.
\end{aligned} \tag{8}$$

To first order there is a positive σ_{22} surface force at the domain wall. This is modelled by a number of forces acting perpendicular to the surface. In the first domain wall shown in figure 6 this force causes an increase in the magnitude of the shear strain close to the surface (i.e. a widening of the domain wall). The reduction of the shear strain results in a positive $(\sigma_{11}+\sigma_{22})$ stress at the surface, which is modelled by two lateral forces on either side of the domain wall. Similarly in the second domain wall shown, the first order force causes a reduction in the magnitude of the shear strain close to the surface, making the domain wall narrower. This increase in the magnitude of the shear strain causes a negative $(\sigma_{11}+\sigma_{22})$ surface stress, again modelled by two lateral forces. The magnitudes and points of action of the forces used are shown in figure 6 and table 4.

The resulting strain profile for the first domain wall is given in figures 7(a)–(c). Similarly the strain profiles for the second wall are given in figures 7(d)–(f). These pictures show a number of similarities to those observed in the numerical calculations. In particular the form of ε_{12} close to both surfaces is reproduced. The calculated form of ε_{22} is also very close to the form found numerically. The reproduction of the form of ε_{11} is not quite so good. Although

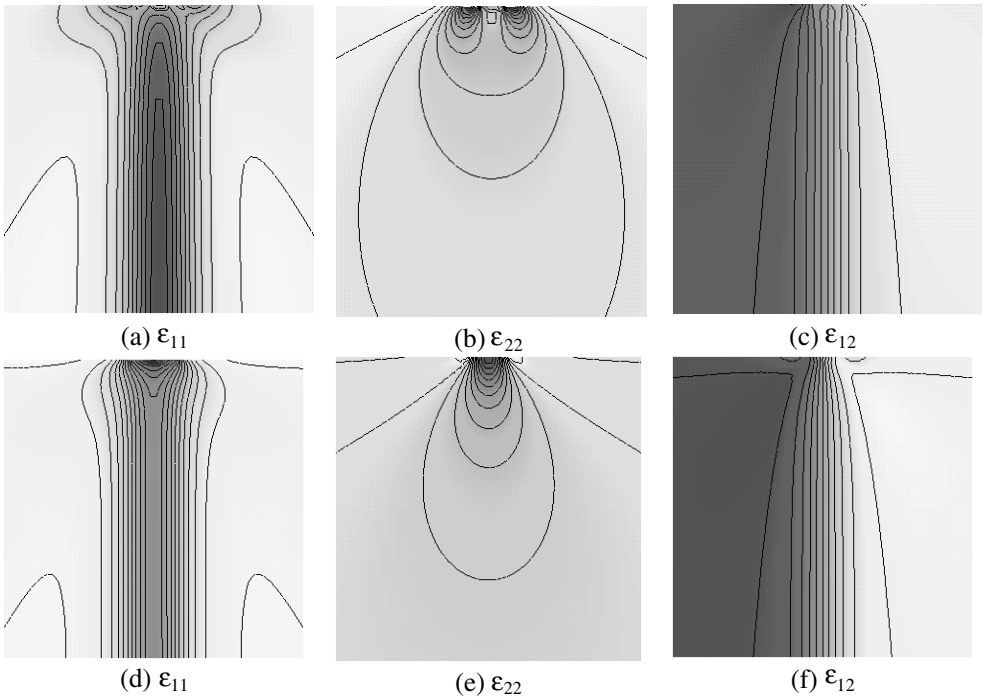

Figure 7. Strains resulting from the surface forces shown in figure 5.

the domain walls show asymmetry it is not quite as large as that seen in the numerical work. Overall, however, the qualitative agreement is good.

4. Conclusions

The effect of the domain wall pressure on the surface structure of a domain wall has not been taken into account in previous models. Its effect is to make the surface structure of the domain wall asymmetric: a domain wall's structure on two opposite sides of a crystal will not be the same.

Acknowledgment

The authors wish to acknowledge funding from the German Research Foundation.

References

Aird A and Salje E K H 1998 Sheet superconductivity in domain walls: experimental evidence in WO_{3-x} *J. Phys.: Condens. Matter* **10** L337–80

Aird A and Salje E K H 2000 Enhanced reactivity of domain walls in WO_3 with sodium *Eur. Phys. J.* B **15** L205–10

Conti S and Salje E K H 2001 Surface structure of ferroelastic domain walls: a continuum elasticity approach *J. Phys.: Condens. Matter* **13** L847–54

Landau L D and Lifshitz E M 1986 *Theory of Elasticity* (Oxford: Butterworth-Heinemann)

Lee W T, Salje E K H and Bismayer U 2001 Structure and transport properties of ferroelastic domain walls in a simple model *Phase Transit.* at press

Novak J and Salje E K H 1998 Surface structure of domain walls *J. Phys.: Condens. Matter* **10** L359–66